MOTIVECTION
Journal of Mechanical Electrical and Industrial Engineering

Volume: 8, Number: 2, 2026
ISSN: 2655 – 7215 [printed] ; 2685-2098 [online]
DOI: https://doi.org/10.46574/motivection.v8i2.543

EMEIRS

Counterweight Reinforcement versus Slope Geometry Redesign for the Block 16 Sidewall at PT XYZ

Bambang Heriyadi[1*], Rinaldo Maretto Patar Simangunsong[1], Yozsi Mingsi Aneperta[1], Heri Prabowo[1], Fariz Aditya[1]

ABSTRACT

Landslides occurred on the Block 16 sidewall at PT XYZ, where the upper benches comprise low-stability fill and the lower benches comprise bedded rock. This study characterized the rock mass, assessed discontinuity-controlled failure potential, calibrated the failed-slope condition by back analysis, and compared counterweight reinforcement with slope-geometry redesign. Scanline mapping, Rock Mass Rating (RMR), stereographic kinematic analysis, Slope Mass Rating (SMR), and Bishop-simplified limit-equilibrium simulations in Slide 6.0 were applied. The lower rock benches had an average RMR of 69.5 and an SMR of 68.6. Oblique-toppling criteria were satisfied by 7.62% of the analyzed discontinuities. The initial model yielded an SF of 1.239, while back analysis reproduced the failure condition at SF = 0.995. Counterweighting increased SF to 1.324 using 42.6 m^3/m of fill; geometry redesign produced SF = 1.352 with 264.98 m^3/m of excavation. Both alternatives met the SF > 1.3 criterion, but counterweighting required substantially less material handling.

Keywords
back analysis; counterweight reinforcement; limit equilibrium; rock mass classification; slope geometry redesign

[1] Department of Mining Engineering, Faculty of Engineering, Universitas Negeri Padang
Jl. Prof Dr. Hamka UNP Air Tawar Padang Campus, Indonesia-25131

* Corresponding Author: bambangh@ft.unp.ac.id

Submitted : April 12, 2026. Accepted : June 07, 2026. Published : August 04, 2026

INTRODUCTION

Indonesia's coal reserves were reported at 38.84 billion t in 2021, with Kalimantan accounting for 62.1% of the national total [1]. Open-pit extraction of these resources requires the progressive removal of overburden and the formation of pit walls, sidewalls, benches, and disposal slopes. Because mine plans and operating sequences continuously change the geometry and loading conditions of these slopes, geotechnical stability must be incorporated into short-term and long-term mine design [2].

Slope-stability assessment in open-pit mines commonly combines rock-mass classification, structural analysis, and numerical or limit-equilibrium modeling. RMR-based characterization provides a systematic description of rock-mass quality, whereas stereographic and kinematic analyses identify whether discontinuity orientations satisfy the geometric conditions for planar, wedge, or toppling failures [3]-[5]. Limit-equilibrium analysis then quantifies the balance between driving and resisting forces for a defined slope geometry and material model [6]. These methods are complementary: classification and kinematic analysis describe the lower rock benches, while numerical analysis can represent the fill-dominated upper benches and the overall potential failure surface.

Field observations at the Block 16 sidewall of PT XYZ in Sangasanga Subdistrict, Kutai Kartanegara Regency, East Kalimantan, identified repeated slope failures. Benches 1 and 2 consist mainly of placed fill, whereas Benches 3 and 4 expose in situ sandstone, claystone, siltstone, and coal seams. The four-bench slope has bench widths of approximately 3-4 m, typical bench heights of about 9 m, and bench angles of 32°-36°. Rainfall increased during early 2025, and the combined influence of fill degradation, precipitation, and mining activity was considered relevant to the observed instability.

Two practical stabilization alternatives were considered. A toe counterweight increases resisting force by adding mass near the slope toe, an approach that has improved stability in embankments and weak-strata mine slopes [7], [8]. By contrast, slope-geometry redesign reduces driving force by flattening or removing part of the slope mass. Such redesign must be evaluated together with earthwork volume and mine-layout constraints because geometric compliance can require substantial cut-and-fill operations [9], [10]. Indonesian good-mining-practice guidance uses an SF criterion greater than 1.3 for the evaluated static slope condition [11].

Previous studies have examined rock-mass classification, kinematic failure potential, counterweight stabilization, and mine-geometry redesign, but the relative material requirement of counterweighting and geometry modification is rarely compared for the same failed sidewall and calibrated material condition. Accordingly, this study aims to (1) characterize the lower rock benches using RMR, kinematic analysis, and SMR; (2) calibrate the fill-dominated failure condition through back analysis; and (3) compare the safety factors and material volumes of counterweight reinforcement and slope-geometry redesign. The comparison is limited to geotechnical performance and material-handling volume; it is not a full life-cycle cost analysis.

METHOD

Study Design and Workflow

The study combined field mapping, company geotechnical data, rock-mass classification, kinematic analysis, back analysis, and limit-equilibrium modeling. Figure 1 organizes the procedure from field diagnosis through the comparison of reinforcement alternatives. Primary data comprised the actual slope geometry, scanline measurements, lithological observations, discontinuity orientations, and field indications of groundwater. Secondary data comprised physical and mechanical material properties, rainfall records, and existing slope-design information supplied by PT XYZ. The analyses were conducted for the Block 16 sidewall, with rock-mass classification focused on Benches 3 and 4 and overall stability modeling focused on the fill-dominated Benches 1 and 2 together with the underlying rock units.

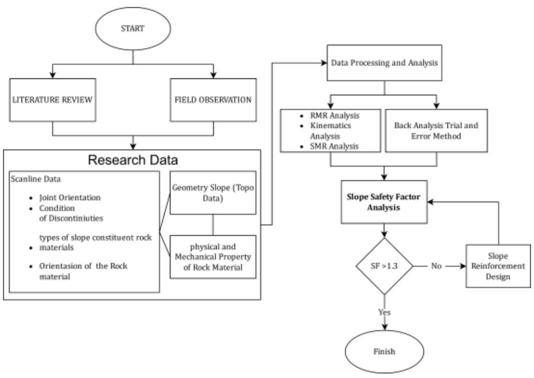

Figure 1. Research workflow for slope characterization, back analysis, reinforcement modeling, and alternative comparison.

Scanline Mapping and Rock-Mass Characterization

A 50 m scanline was established along the exposed rock face to record discontinuity orientation, spacing, condition, and lithological context. Scanline mapping is widely used to characterize fractured rock masses, although representativeness depends on exposure quality and geological variability [12]. The measured discontinuities were used to determine RQD-related ratings, discontinuity spacing, discontinuity condition, and structural orientations. Because the exposed section showed broadly similar roughness and lithological conditions along the observation line, the scanline was treated as representative of the observed lower sidewall section.

RMR was calculated using intact-rock strength, RQD, discontinuity spacing, discontinuity condition, and groundwater condition. The adopted rating ranges are summarized in Table 1, and the resulting classes are interpreted using Table 2. The system follows the Bieniawski RMR framework [13], while recent correlation studies illustrate its continued use across sandstone, siltstone, granite, and quartzite rock masses [14].

Table 1. RMR parameters and ratings adopted in the study [13].

Parameter	Criterion or range	Rating
Point-load index, MPa	>10; 10-4; 4-2; 2-1	15; 12; 7; 4
Uniaxial compressive strength, MPa	>250; 100-250; 50-100; 25-50; 5-25; 1-5; <1	15; 12; 7; 4; 2; 1; 0
RQD, %	90-100; 75-90; 50-75; 25-50; <25	20; 17; 13; 8; 3
Discontinuity spacing, m	>2; 0.6-2; 0.2-0.6; 0.06-0.2; <0.06	20; 15; 10; 8; 5
Discontinuity condition	Very rough, discontinuous, no separation, unweathered; slightly rough, separation <1 mm, slightly weathered; slightly rough, separation <1 mm, highly weathered; slickensided or gouge <5 mm / separation 1-5 mm, continuous; soft gouge >5 mm / separation >5 mm, continuous	30; 25; 20; 10; 0
Groundwater inflow, L/min per 10 m	None; <10; 10-25; 25-125; >125	15; 10; 7; 4; 0
Joint-water-pressure ratio	0; <0.1; 0.1-0.2; 0.2-0.5; >0.5	15; 10; 7; 4; 0
General groundwater condition	Completely dry; damp; wet; dripping; flowing	15; 10; 7; 4; 0

Table 2. RMR class interpretation [13].

RMR	Class	Rock-mass quality	Cohesion (kPa)	Friction angle
81-100	I	Very good	>400	>45°
61-80	II	Good	300-400	35°-45°
41-60	III	Fair	200-300	25°-35°
21-40	IV	Poor	100-200	15°-25°
<21	V	Very poor	<100	<15°

Stereographic Kinematic Analysis and SMR

The measured slope and discontinuity orientations were plotted stereographically to evaluate the geometric feasibility of structurally controlled failure. Stereographic projection transfers three-dimensional orientation data to a two-dimensional net, allowing discontinuity sets to be compared with the slope face and friction constraints [15]. The kinematic criteria were interpreted with reference to documented applications to rock slopes and quarry faces [15], [16].

SMR was calculated by adjusting the basic RMR value for the relationship between discontinuity orientation, slope orientation, and excavation method. The correction-factor criteria are given in Table 3, the excavation-method rating is given in Table 4, and the final SMR class is interpreted using Table 5. This approach follows the Romana formulation as applied in recent slope assessments [17].

Table 3. SMR orientation correction factors.

Failure mode	Factor	Criterion	Criterion categories	Ratings
Planar (P)	F1	|α1 - α2|	>30° / 30°-20° / 20°-10° / 10°-5° / <5°	0.15 / 0.40 / 0.70 / 0.85 / 1.00
Toppling (T)	F1	|α1 - α2 - 180°|	>30° / 30°-20° / 20°-10° / 10°-5° / <5°	0.15 / 0.40 / 0.70 / 0.85 / 1.00
Planar (P)	F2	|β1|	<20° / 20°-30° / 30°-35° / 35°-45° / >45°	0.15 / 0.40 / 0.70 / 0.85 / 1.00
Toppling (T)	F2	-	All criteria	1.00
Planar (P)	F3	β1 - β2	>10° / 10°-0° / 0° / 0° to -10° / <-10°	0 / -6 / -25 / -50 / -60
Toppling (T)	F3	β1 + β2	<100° / 110°-120° / >120°	0 / -6 / -25

α1 = slope dip direction; α2 = discontinuity strike or dip direction as defined in the adopted SMR convention; β1 = discontinuity dip; β2 = slope dip.

Table 4. Excavation-method rating (F4).

Excavation method	F4
Natural slope	15
Presplitting blasting	10
Smooth blasting	8
Normal blasting	0
Deficient blasting	-8
Mechanical excavation	0

Table 5. SMR class interpretation.

Class	SMR	Rock-mass quality	Stability	Typical failure	Failure probability
I	81-100	Very good	Completely stable	No failure	0
II	61-80	Good	Stable	Some block failure	0.2
III	41-60	Normal	Partially stable	Planar, joint, or wedge	0.4
IV	21-40	Bad	Unstable	Planar or large wedge	0.6
V	0-20	Very bad	Completely unstable	Large planar or soil-like/circular	0.9

The SMR value was calculated using Equation (1), where RMR is the basic rock-mass rating and F1-F4 are the orientation and excavation corrections.

$$SMR = RMR + (F_1 X F_2 X F_3) + F_4 \quad (1)$$

Back Analysis and Limit-Equilibrium Modeling

Back analysis was used to infer the fill-material shear-strength parameters associated with the observed failure condition. The procedure compared the modeled safety factor with the field evidence of instability and iteratively adjusted cohesion and friction angle while holding the documented geometry and other material units constant. Figure 2 summarizes this inverse process. Back analysis is inherently model-dependent because the inferred parameters are conditional on the selected failure mechanism, geometry, pore-pressure assumption, and analytical method [18], [19]. A comparable trial-and-error approach has been applied to mine-slope failures to derive engineering parameters for stabilization design [20].

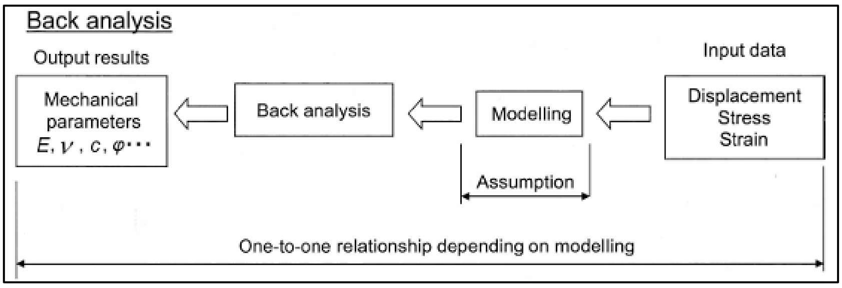

Figure 2. Depiction of Backward Analysis

Slope stability was evaluated in Slide 6.0 using the Bishop-simplified limit-equilibrium method. The analysis used the documented cross-section and material units. The field inspection identified no seepage or exposed groundwater in the study area; therefore, the model did not include an observed groundwater surface. The safety factor represents the ratio of available resisting capacity to mobilized driving demand for the assumed slip surface and material model [21].

Reinforcement Alternatives and Comparison Criterion

The calibrated failure-condition parameters were used to evaluate two alternatives. In the counterweight model, claystone fill was placed at the slope toe to increase resisting force without changing the principal upper-slope geometry. Figure 3 illustrates the stabilizing mechanism. In the geometry-redesign model, slope material was removed to reduce the driving mass and flatten the overall profile. Both alternatives were iteratively configured until the modeled SF exceeded 1.3, consistent with the adopted regulatory criterion [11]. Their material requirements were then calculated per metre of slope length and compared directly. Counterweight performance can be sensitive to toe geometry, foundation response, and material properties, as shown in numerical studies of loaded or undercut slopes [22].

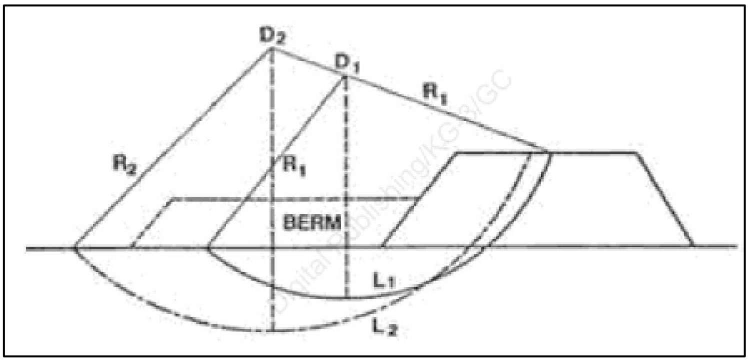

Figure 3. Counterweight Structure on Slopes

RESULTS AND DISCUSSION

Results

Geological and Geometric Conditions

The Block 16 sidewall comprises four benches and two principal material domains. Benches 1 and 2 are formed mainly by dump fill, whereas Benches 3 and 4 comprise layered sandstone, claystone, siltstone, and coal. Figure 4 shows the cross-section used to distinguish the fill from the original rock sequence and to establish the geometry for subsequent analyses.

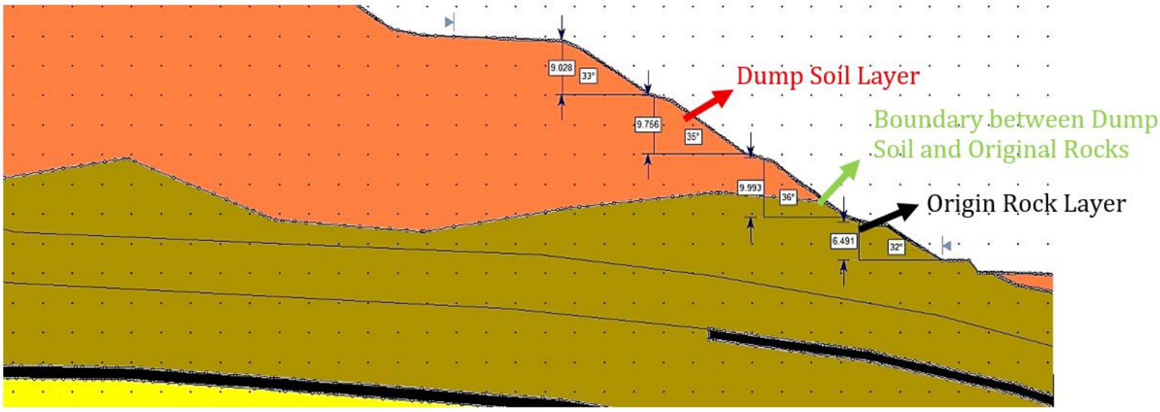

Figure 4. Actual Block 16 sidewall cross-section showing the dump-fill layer, original rock units, and their boundary (source: PT XYZ model data).

Sandstone is the dominant exposed lithology, particularly in the eastern part of the pit. It is light brown, 15-20 m thick, and oriented N 356°E/24°E. Claystone is blackish brown, 10-16 m thick, and oriented N 6°E/28°E. Coal seam A4 is approximately 3 m thick and oriented N 354°E/28°E. The physical and mechanical properties supplied by PT XYZ for the lower benches are listed in Tables 6 and 7.

Table 6. Physical properties of materials in Benches 3 and 4 (source: PT XYZ geotechnical drilling).

No.	Material	Density (g/cm^3)	Unit weight (kN/m^3)
1	Claystone	2.18	21.38
2	Sandstone	2.36	23.14
3	Coal	1.30	12.75

Table 7. Uniaxial compressive strength of materials in Benches 3 and 4 (source: PT XYZ geotechnical drilling).

No.	Material	UCS (MPa)
1	Claystone	7.23
2	Sandstone	7.40
3	Coal	9.10

Scanline Mapping and RMR

The scanline geometry and location are summarized in Table 8. The 50 m line crossed the exposed lower sidewall at a slope strike of N 70°E and a slope dip of 40°. Figure 5 shows the mapped discontinuity traces in relation to the lithological units. Thirteen fractures were recorded in sandstone and two in claystone. This count indicates a greater observed discontinuity frequency in sandstone along the scanline; it does not by itself establish lower intact-rock strength.

Table 8. Scanline measurement geometry and location.

Parameter	Value
Slope height	10 m
Slope strike	N 70°E
Slope dip	40°
Scanline length	50 m
Scanline strike	N 214°E
Scanline dip	5°
Coordinates	50S / 0527739 / 9926540

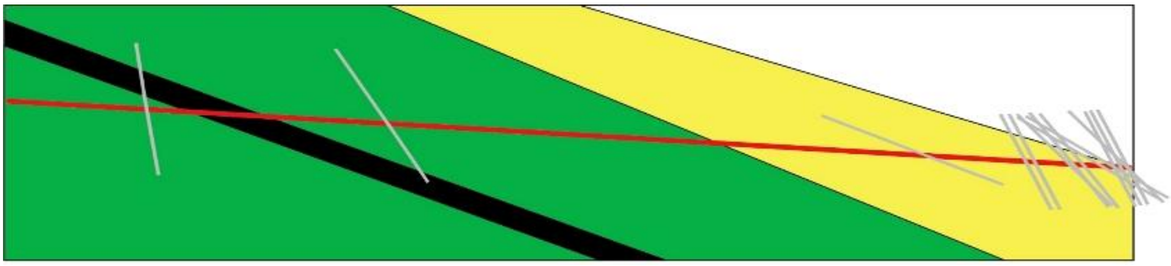

Figure 5. Mapped discontinuity traces in the sandstone, claystone, and coal sequence of Benches 3 and 4 (source: field scanline interpretation).

The RMR ratings are presented in Table 9. Claystone obtained a total rating of 72 and sandstone a rating of 67, producing an average RMR of 69.5. This average lies in Class II (good rock). The result describes the observed lower rock benches and should not be generalized to the dump fill in Benches 1 and 2.

Table 9. RMR scoring for the mapped lower-bench lithologies.

No.	Lithology	Point-load index	RQD	Joint spacing	Joint condition	Ground water	Total
1	Claystone	2	20	20	20	10	72
2	Sandstone	2	20	15	20	10	67
			Average RMR				**69.5**

Kinematic and SMR Results

Stereographic projection identified a slope orientation of N 70°E/40° and two joint sets: JS1 at N 346°E/70° and JS2 at N 187°E/70°. Figure 6 plots the slope and joint orientations. The relationship between JS2 and the slope face satisfies part of the geometric condition for toppling. The kinematic envelope in Figure 7 shows that 7.62% of the analyzed discontinuity orientations fall within the oblique-toppling critical zone, with an indicated direction of N 97°E.

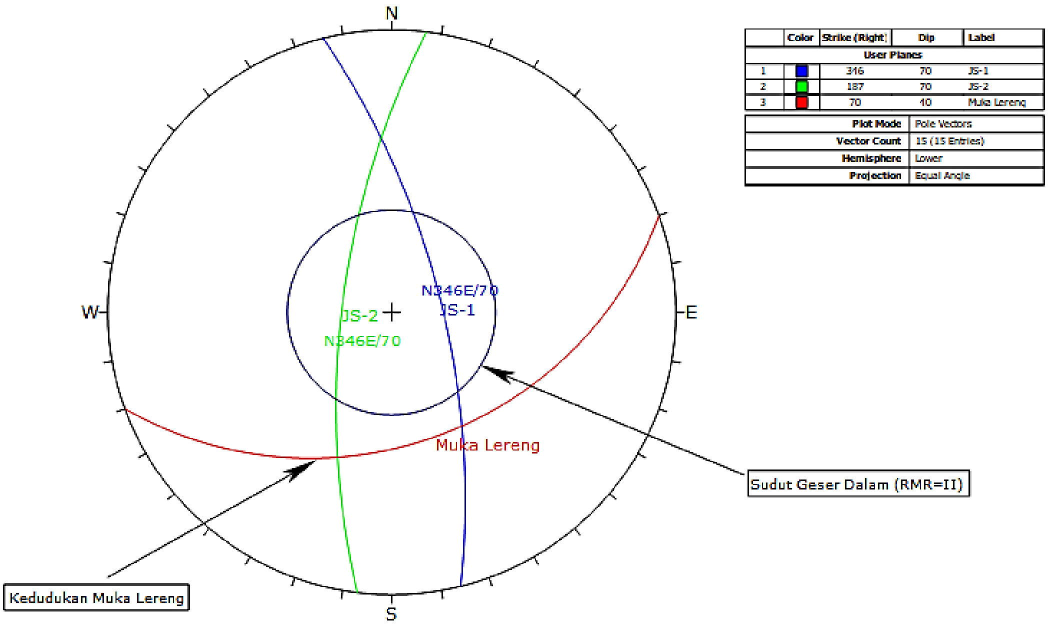

Figure 6. Stereographic projection of the Block 16 sidewall and measured joint-set orientations (source: Dips analysis).

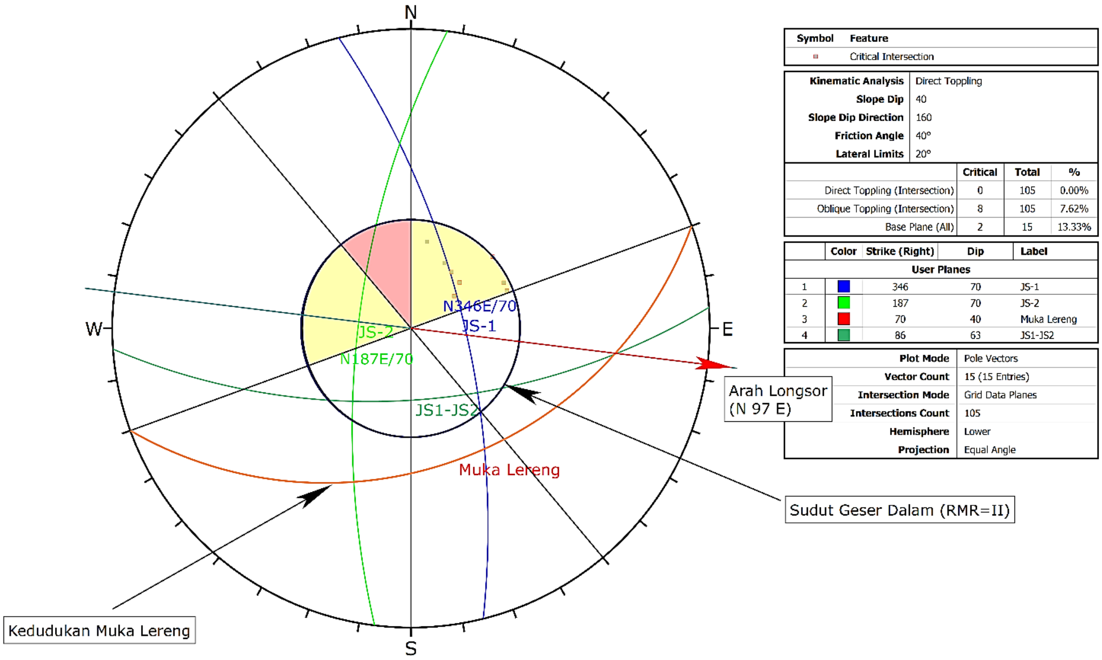

Figure 7. Kinematic oblique-toppling analysis for the Block 16 sidewall (source: Dips analysis).

The SMR input geometry is listed in Table 10, and the selected correction ratings are listed in Table 11. Substituting the average RMR and correction ratings into Equation (1) gives the SMR calculation in Equation (2).

Table 10. SMR orientation components used in the calculation.

Component	Value
Slope dip direction (α1)	N 160°E
Joint strike/direction (α2)	N 277°E
Joint dip (β1)	70° (JS2)

Component	Value
Slope dip (β2)	40°

Table 11. SMR correction ratings selected for the analyzed toppling condition.

Factor	Calculated or selected value	Rating
F1	200°	0.15
F2	70°	1.00
F3	110°	-6
F4	Mechanical excavation	0

$$\text{SMR} = 69.5 + (0.15 + 1 \text{ x } (-6)) + 0 = 68.6 \quad (2)$$

The resulting SMR of 68.6 is Class II, corresponding to a good rock mass and a generally stable rock-slope condition under the adopted classification. This classification again applies to the lower rock benches and does not replace the overall limit-equilibrium analysis of the fill-controlled sidewall.

Back Analysis of the Fill-Dominated Failure

The material parameters initially used by PT XYZ are listed in Table 12. No visible seepage or groundwater opening was observed during field data collection. Using these parameters and the documented geometry, the initial Bishop-simplified model produced SF = 1.239, as shown in Figure 8. Although the modeled slope had not reached limiting equilibrium, the result remained below the adopted SF > 1.3 criterion.

Table 12. Material properties used in the initial PT XYZ slope model.

Material	Bulk unit weight (kN/m^3)	Saturated unit weight (kN/m^3)	Cohesion (kPa)	Friction angle
Dump fill	18.0	-	26.0	18.00°
Siltstone	22.6	24.0	122.0	22.17°
Sandstone	22.5	23.9	62.75	35.36°
Coal	13.4	13.5	45.0	5.00°

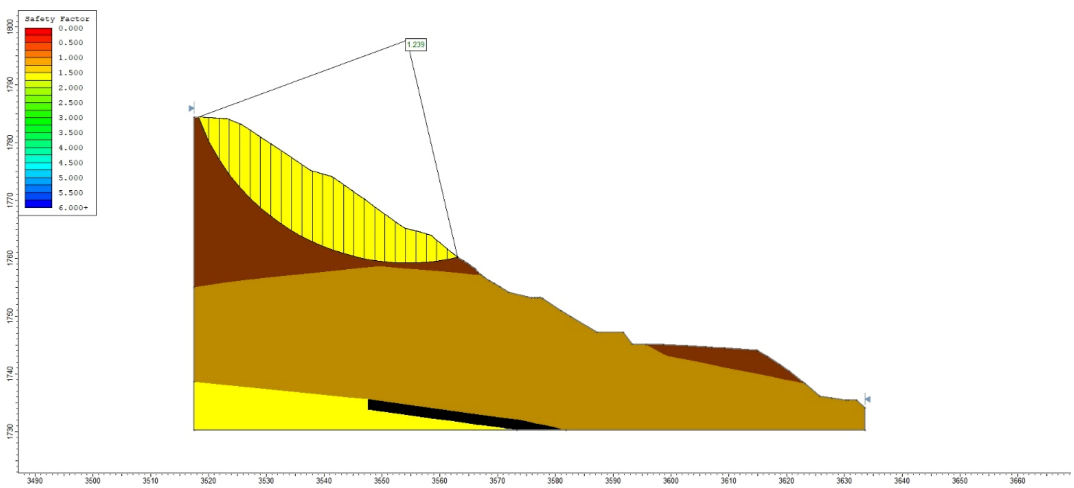

Figure 8. Initial limit-equilibrium model using company material parameters; Bishop-simplified SF = 1.239 (source: Slide 6.0 analysis).

Back analysis progressively reduced the dump-fill cohesion and friction angle while the documented geometry and other material units were retained. Table 13 shows that the modeled SF decreased from 1.157 to 1.076 and finally to 0.995. The third trial was therefore adopted as the calibrated failure condition, with dump-fill cohesion of 20 kPa and friction angle of 15°.

Table 13. Trial-and-error back-analysis results for the dump fill.

Trial	Material	Cohesion (kPa)	Friction angle	SF
1	Dump fill	24	17°	1.157
2	Dump fill	22	16°	1.076
3	Dump fill	20	15°	0.995

Counterweight Reinforcement

Claystone available near seams A8 and A9 in the lowwall of Blocks 12-13 was selected as the counterweight material. Its properties and the properties of the retained rock units are listed in Table 14. The counterweight geometry was modeled at the slope toe using the back-calibrated dump-fill parameters.

Table 14. Material properties used in the counterweight-reinforced model.

Material	Unit weight (kN/m^3)	Cohesion (kPa)	Friction angle
Claystone counterweight	22.2	176.0	22.81°
Sandstone	22.5	62.7	35.45°
Siltstone	22.6	112.0	22.16°

The Bishop-simplified analysis in Figure 9 produced a minimum SF of 1.324, which exceeds the adopted criterion. Figure 10 shows a counterweight cross-sectional area of 42.6 m^2; for a one-metre longitudinal slice, this corresponds to 42.6 m^3/m of fill.

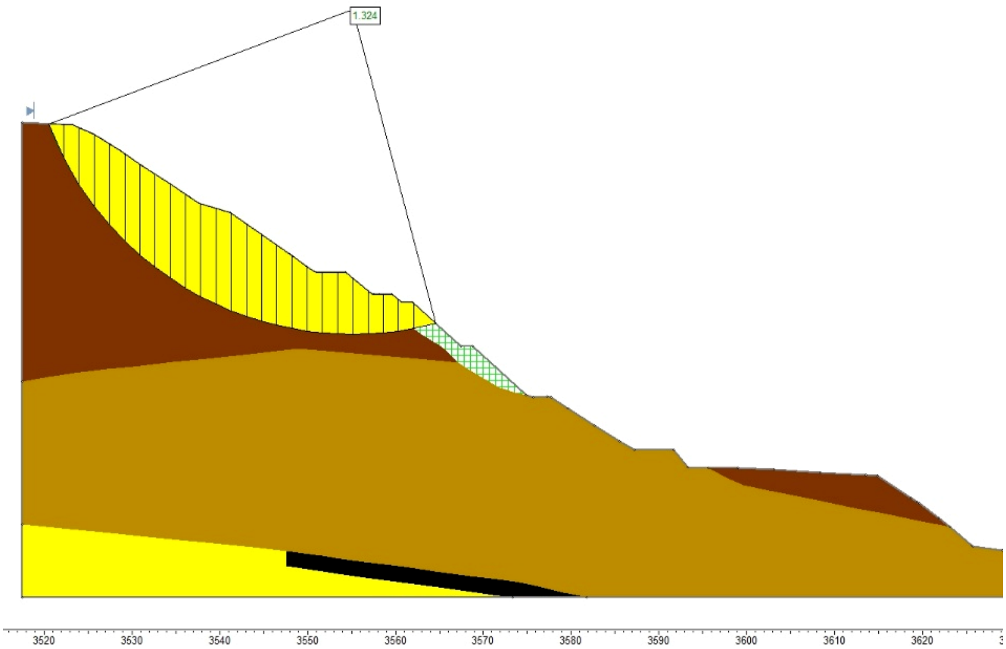

Figure 9. Counterweight-reinforced slope model; Bishop-simplified minimum SF = 1.324 (source: Slide 6.0 analysis).

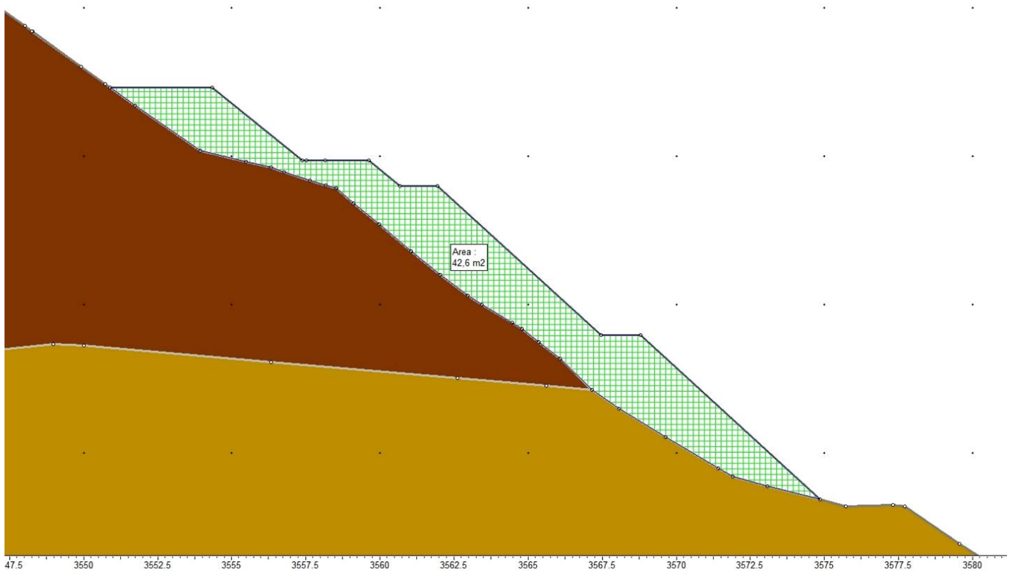

Figure 10. Counterweight geometry with a cross-sectional area of 42.6 m^2 (source: Slide 6.0 geometry model).

Slope-Geometry Redesign

The alternative redesign reduced the driving mass by trimming and flattening the sidewall geometry. The redesigned cross-section is shown in Figure 11. Limit-equilibrium analysis of this geometry produced SF = 1.352 (Figure 12), which also exceeds the adopted criterion. The cut area shown in Figure 13 is 264.98 m^2, corresponding to 264.98 m^3/m of excavated material for a one-metre longitudinal slice.

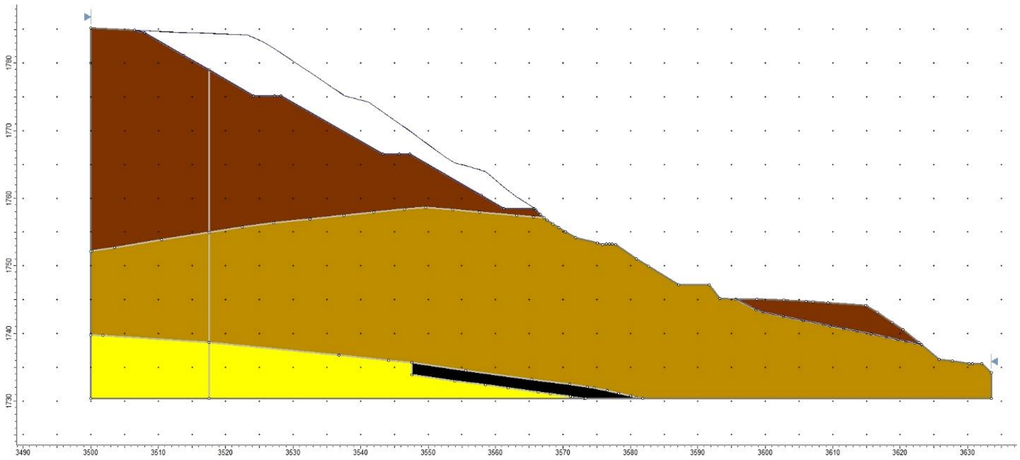
Figure 11. Block 16 sidewall geometry after slope redesign (source: Slide 6.0 geometry model).

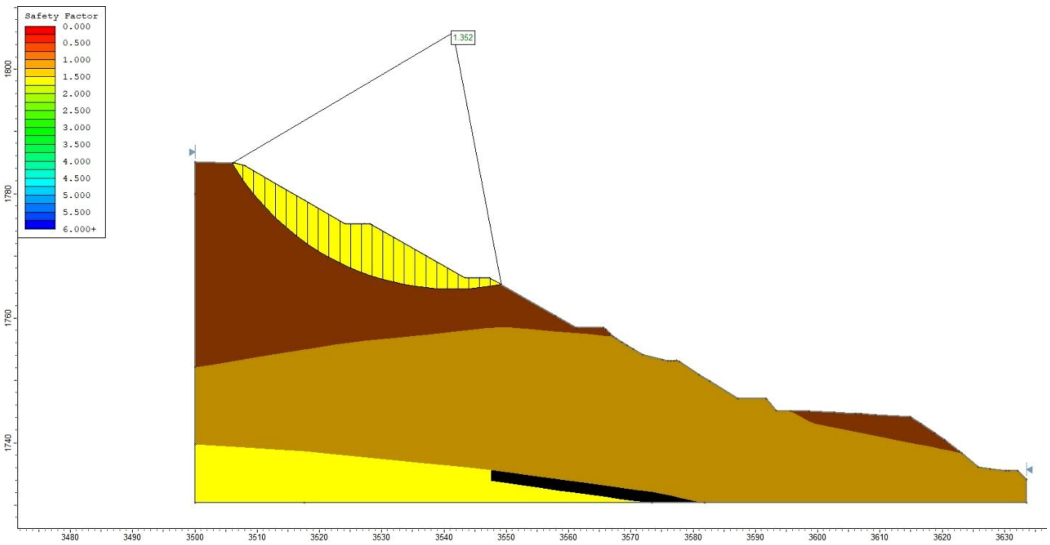

Figure 12. Redesigned slope model; Bishop-simplified SF = 1.352 (source: Slide 6.0 analysis).

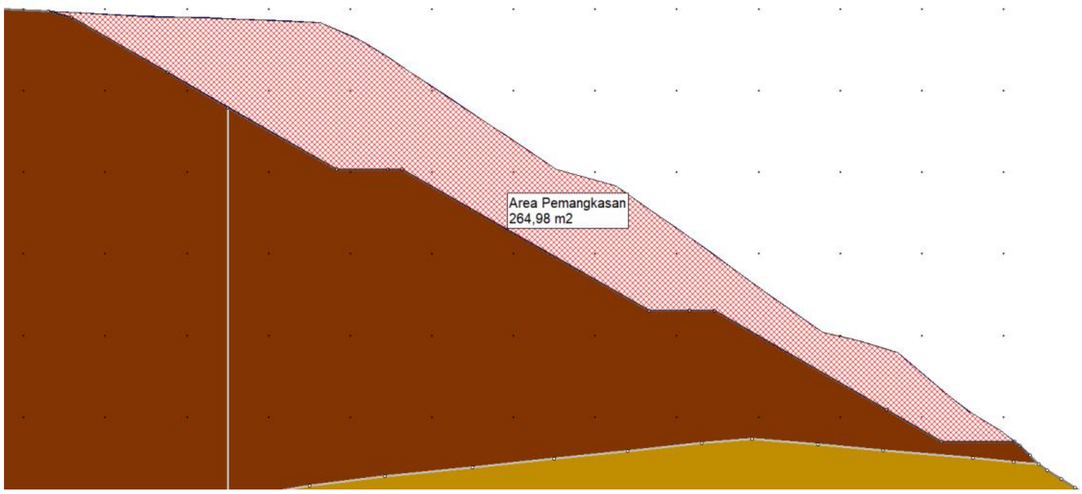

Figure 13. Geometry of the material removed in the slope-redesign alternative; cut area = 264.98 m^2 (source: geometry calculation).

Comparison of the Reinforcement Alternatives

Table 15 compares the two alternatives on the same performance and volume basis. Counterweight reinforcement yielded SF = 1.324 with 42.6 m^3/m of added material, whereas geometry redesign yielded SF = 1.352 with 264.98 m^3/m of excavated material. Both met the adopted stability criterion, but the counterweight alternative required much less material handling for the analyzed cross-section.

Table 15. Safety-factor and material-volume comparison of the two stabilization alternatives.

Alternative	SF	Material action	Volume per metre
Counterweight reinforcement	1.324	Fill placement	42.6 m^3/m
Slope-geometry redesign	1.352	Excavation	264.98 m^3/m

Discussion

Rock-Mass and Structural Interpretation

The average RMR of 69.5 and SMR of 68.6 indicate that the mapped lower benches contain generally good rock mass. This result is consistent with mine-slope studies in which RMR values in the upper-50s to mid-70s represent fair-to-good rock conditions [3], [4]. The classification does not conflict with the observed sidewall failure because the failed upper benches are dominated by placed fill, whereas RMR and SMR were derived from the original rock exposed in Benches 3 and 4. The distinction between these material domains is therefore essential: classification of the lower rock cannot be used as evidence that the entire composite slope is stable.

The 7.62% kinematic result should be interpreted as the proportion of analyzed orientations that satisfy the oblique-toppling criteria, not as a time-based probability that failure will occur. Figure 7 indicates a structurally plausible but limited toppling component in the lower rock benches. Similar stereographic applications emphasize that kinematic feasibility identifies potential failure modes, while actual instability also depends on persistence, shear strength, water pressure, geometry, and loading [5], [15], [16]. In the present case, the overall sidewall instability is more directly represented by the fill-controlled limit-equilibrium model than by the lower-bench toppling envelope alone.

Back-Analysis Implications

The initial SF of 1.239 in Figure 8 already fell below the adopted 1.3 criterion, indicating inadequate margin under the company parameter set. The back-analysis sequence in Table 13 reduced the dump-fill shear strength until SF approached unity, producing a calibrated condition of c = 20 kPa, φ = 15°, and SF = 0.995. This result is coherent with the observed failure state and illustrates the principal value of back analysis: parameters are inferred from field behavior rather than accepted solely from pre-failure design assumptions [18]-[20].

The calibrated values should nevertheless be regarded as equivalent parameters for the selected two-dimensional model, not unique intrinsic properties. Back-analysis solutions depend on the assumed slip surface, pore-pressure condition, constitutive simplification, and analytical method [18], [19], [21]. The absence of visible seepage justified the adopted groundwater assumption for the analyzed observation period, but it does not exclude transient pore-pressure development during heavy rainfall. Parameter uncertainty and rainfall-dependent hydraulic response therefore remain important sources of model risk.

Performance of Counterweighting and Geometry Redesign

Both stabilization alternatives raised the calculated SF above 1.3. The counterweight model in Figure 9 achieved SF = 1.324 by increasing resisting force at the toe, whereas the redesigned profile in Figure 12 achieved SF = 1.352 by reducing the driving mass and flattening the geometry. These mechanisms agree with the established behavior of counterweight fills and geometry-based stabilization [7], [8], [22]. The modest difference between the two final SF values indicates that both configurations were designed close to the same minimum acceptance criterion rather than to maximize SF.

The main practical difference is the material requirement summarized in Table 15. The counterweight alternative used 42.6 m^3/m of fill, while the geometry-redesign alternative required 264.98 m^3/m of excavation. This finding supports counterweighting as the more material-volume-efficient option for the analyzed section. It also aligns with broader mine-design studies showing that geometric redesign must be evaluated together with earthwork requirements and operational constraints [9], [10]. However, the present comparison does not quantify haul distance, equipment hours, drainage works, construction sequencing, land availability, or long-term maintenance. Consequently, the result supports a volume-based preference rather than a complete economic ranking.

The counterweight recommendation is also conditional on material quality and foundation performance. Counterweight behavior is sensitive to the unit weight, shear strength, placement geometry, and interaction with the underlying toe material [8], [22]. The claystone properties used in Table 14 produced an acceptable modeled SF, but field implementation should verify the actual borrow material, compaction condition, drainage, and construction geometry. Monitoring after placement would be required to confirm that the modeled stability margin is maintained under rainfall and mining-induced disturbance.

CONCLUSION

The Block 16 sidewall contains two geotechnically distinct domains: generally good lower rock benches and unstable fill-dominated upper benches. The lower rock mass had an average RMR of 69.5 and an SMR of 68.6, while 7.62% of the measured discontinuity orientations satisfied the adopted oblique-toppling criteria. The initial limit-equilibrium model produced SF = 1.239, and back analysis reproduced the observed failure condition at SF = 0.995 using dump-fill cohesion of 20 kPa and a friction angle of 15°. Counterweight reinforcement increased SF to 1.324 with 42.6 m^3/m of fill, whereas slope-geometry redesign increased SF to 1.352 with 264.98 m^3/m of excavation. Both alternatives met the adopted SF > 1.3 criterion, but counterweighting required considerably less material handling and is therefore the preferred alternative for the analyzed cross-section on a volume basis.

This preference remains conditional on verification of the counterweight material, toe-foundation condition, drainage performance, and construction quality. Future work should include laboratory or field testing of the proposed counterweight fill, rainfall-sensitive groundwater assessment, parameter-uncertainty analysis, and post-construction monitoring before the design is generalized to other sections of the sidewall.

REFERENCES

[1] Kementerian Energi dan Sumber Daya Mineral Republik Indonesia, “Cadangan batubara masih 38,84 miliar ton, teknologi bersih pengelolaannya terus didorong,” Jul. 26, 2021. [Online]. Available: https://www.esdm.go.id/id/media-center/arsip-berita/cadangan-batubara-masih-3884-miliar-ton-teknologi-bersih-pengelolaannya-terus-didorong. Accessed: Jul. 20, 2026.

[2] M. Blom, A. R. Pearce, and P. J. Stuckey, “Short-term planning for open pit mines: A review,” Int. J. Min. Reclam. Environ., vol. 33, no. 5, pp. 318-339, 2019, doi: 10.1080/17480930.2018.1448248.

[3] F. Aditya, B. Heriyadi, T. G. Saldy, F. Nauli, S. R. Yanti, R. Marlina, K. E. Putra, R. Algozi, and M. Akmal, “Mine slope stability analysis CV. Putra Idola against the Padang-Painan cross road with GSI method and Rock Mass Rating,” MOTIVECTION: J. Mech. Electr. Ind. Eng., vol. 7, no. 2, pp. 129-144, 2025, doi: 10.46574/motivection.v7i2.437.

[4] M. E. F. Kamil, A. B. Manggadyta, and Y. F. Prakoso, “Quantitative assessment for rock mass slope stability in Padalarang mining area, Indonesia using RMR, SMR, and kinematic analysis,” in Proc. 21st New Zealand Geotechnical Society Symp., Dunedin, New Zealand, 2021, pp. 1-8.

[5] C. P. Borja Bernal and L. Jordá Bordehore, “Application of the kinematic assessment of multi-faced slopes using stereographic projection: The case study of a planar failure on the Spondylus Coast, Ecuador,” Appl. Sci., vol. 13, no. 14, Art. no. 8245, 2023, doi: 10.3390/app13148245.

[6] H. Prabowo, I. Suryani, and I. Sabilillah, “Slope stability analysis at disposal mine area using Morgenstern-Price method,” AIP Conf. Proc., vol. 3001, no. 1, Art. no. 100001, 2024, doi: 10.1063/5.0184136.

[7] T. Sakai, S. Inukai, M. Inagaki, and M. Nakano, “Improvement in seismic resistance using replacement/counterweight fill method for existing high embankments on inclined ground constructed with various embankment materials,” Soils Found., vol. 63, no. 2, Art. no. 101284, 2023, doi: 10.1016/j.sandf.2023.101284.

[8] R. A. Nata, G. Ren, Y. Ge, C. Zhang, L. Zhang, H. Panggabean, and V. Syahmer, "Optimizing counterweight backfilling for slope stability in weak strata: An integrated approach combining high-resolution monitoring and numerical modeling," Eng, vol. 6, no. 9, Art. no. 242, 2025, doi: 10.3390/eng6090242.

[9] D. Lestari, S. R. Yanti, T. G. Saldy, and R. A. P. Heriawan, "Geometric redesign and cut-and-fill volume estimation of a non-compliant mine haul road at Pit Banko Tengah A, South Sumatra," MOTIVECTION: J. Mech. Electr. Ind. Eng., vol. 8, no. 2, pp. 125-142, 2026, doi: 10.46574/motivection.v8i2.583.

[10] D. Yulhendra, F. Sandrio, and A. Octova, "Development mine scheduling concept in making pit design," MOTIVECTION: J. Mech. Electr. Ind. Eng., vol. 5, no. 2, pp. 269-282, 2023, doi: 10.46574/motivection.v5i2.208.

[11] Kementerian Energi dan Sumber Daya Mineral Republik Indonesia, Keputusan Menteri Energi dan Sumber Daya Mineral Republik Indonesia Nomor 1827 K/30/MEM/2018 tentang Pedoman Pelaksanaan Kaidah Teknik Pertambangan yang Baik. Jakarta, Indonesia, 2018.

[12] C. Zangerl, M. Koppensteiner, and T. Strauhal, "Semiautomated statistical discontinuity analyses from scanline data of fractured rock masses," Appl. Sci., vol. 12, no. 19, Art. no. 9622, 2022, doi: 10.3390/app12199622.

[13] Z. T. Bieniawski, Engineering Rock Mass Classifications. New York, NY, USA: Wiley, 1989.

[14] G. Somodi, N. Bar, L. Kovács, M. Arrieta, Á. Török, and B. Vásárhelyi, "Study of Rock Mass Rating (RMR) and Geological Strength Index (GSI) correlations in granite, siltstone, sandstone and quartzite rock masses," Appl. Sci., vol. 11, no. 8, Art. no. 3351, 2021, doi: 10.3390/app11083351.

[15] C.-Y. Lee and I.-T. Wang, "Analysis of highway slope failure by an application of the stereographic projection," World Acad. Sci. Eng. Technol. Int. J. Environ. Earth Sci., vol. 5, no. 3, pp. 122-129, 2011.

[16] B. Sirait, Z. Pulungan, and E. Pujianto, "Identifikasi potensi longsoran lereng pada kuari batugamping menggunakan analisis kinematika," J. Teknol. Miner. Batubara, vol. 17, no. 2, pp. 61-75, 2021, doi: 10.30556/jtmb.Vol17.No2.2021.1113.

[17] E. Kalhan and C. Kincal, "Slope stability evaluation of gneiss rock slopes using Slope Mass Rating (SMR) and QSlope," J. S. Afr. Inst. Min. Metall., vol. 125, no. 8, pp. 437-452, 2025, doi: 10.17159/2411-9717/3606/2025.

[18] S. Sakurai, Back Analysis in Rock Engineering. Boca Raton, FL, USA: CRC Press, 2017.

[19] S. P. Parmar, "Contemporary approaches to slope stability back analysis," J. Adv. Geotech. Eng., vol. 8, no. 3, pp. 13-33, 2025, doi: 10.5281/zenodo.15589554.

[20] S. Selsabeel, D. A. Widiarso, and D. Trisnawati, "Analisis balik stabilitas lereng tambang dan rekomendasi rekayasa keteknikannya: Studi kasus area low wall Pit Y Blok 4900-550 Strip 3500-4300 PT Pamapersada Nusantara site PT Adaro Indonesia," J. Geosains Teknol., vol. 4, no. 3, pp. 142-150, 2021, doi: 10.14710/jgt.4.3.2021.142-150.

[21] R. Chowdhury, P. Flentje, and G. Bhattacharya, Geotechnical Slope Analysis. Boca Raton, FL, USA: CRC Press, 2009, doi: 10.1201/9780203864203.

[22] H. Sarfaraz, M. H. Khosravi, and T. Pipatpongsa, "Numerical stability analysis of undercut slopes evaluated by response surface methodology," J. Min. Environ., vol. 12, no. 1, pp. 31-43, 2021, doi: 10.22044/jme.2020.10199.1957.

This page is intentionally left blank.